evaporator, LEED and ion gun before every set of experiments. The base pressure of both the preparation and analysis chambers was less than 2×10^{-10} mbar. The pressure in the preparation chamber was less than 3×10^{-9} mbar during evaporation. LEED was used to characterize the symmetry of the superstructure and XPS to study the dynamics of the interaction between Ge and Pt atoms. It thus also gives information on the nature of the formed superstructure.

3. Results and discussion

3.1. LEED results and analysis

The LEED pattern of the clean Pt(111) is shown in figure 1(a). This is the well-known (1×1) structure of the Pt(111) surface. After Ge deposition, the LEED shows extra spots in addition to those from Pt. It is displayed in figure 1(c). We have made schematic diagrams of the patterns for better understanding. In figure 1(d) it can be seen that the pattern is composed of two symmetrically equivalent domains with the lattice vectors rotated with respect to those of Pt(111). This structure is the same as the one reported by Meng et al. for buckled silicene on Ir(111) [14]. Thus we identified it as a $(\sqrt{7}\times\sqrt{7})$ structure with respect to Pt(111). For brevity it will be called $\sqrt{7}$ throughout this paper.

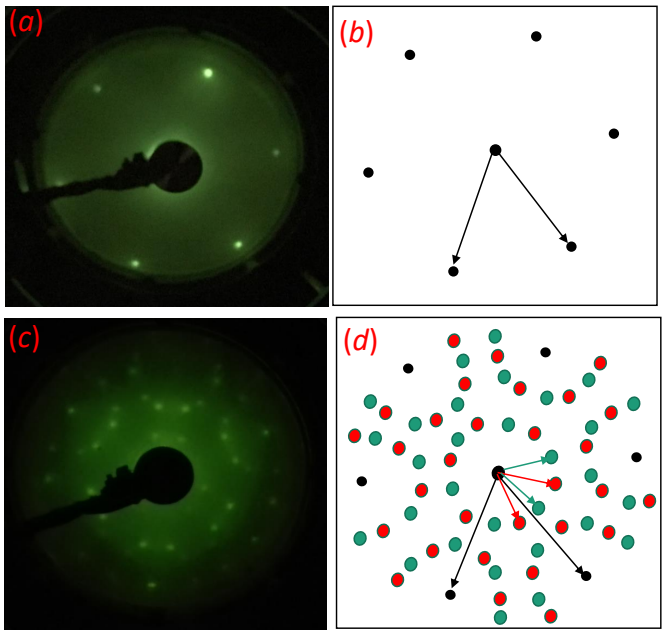

Figure 1. (*a*) LEED image taken at 73 eV of clean Pt(111). (*b*) Schematic diagram of the pattern shown in (*a*). The black arrows are the unit vectors of Pt. (*c*) LEED image taken at 65 eV of Ge/Pt(111). (*d*) Schematic diagram of the LEED pattern of Ge/Pt(111). The red and green arrows are the unit vectors of the two domains formed by Ge.

Upon annealing to 750°C, the structure changed to a new structure displayed in figure 2a. It was composed of two symmetrically equivalent domains with rotated lattice vectors with respect to Pt(111). This is the previously reported $(\sqrt{19}\times\sqrt{19})$ reconstruction formed by Ge on Pt(111) by Li et al., that they ascribed to germanene [10]. We call this structure $\sqrt{19}$ for brevity.

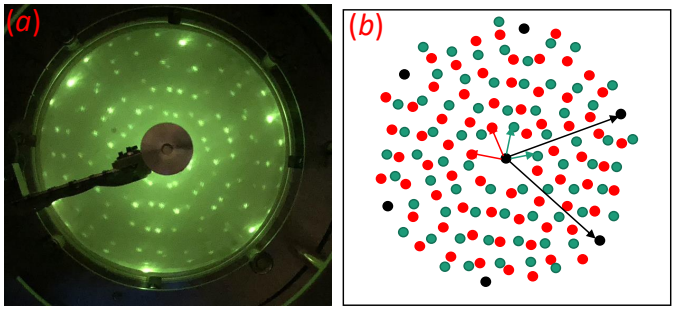

Figure 2. (*a*) LEED image taken at 65 eV of Ge/Pt(111) annealed at 750°C. (*b*) Schematic diagram of the Ge/Pt(111) LEED pattern.

3.2. XPS analysis

Detailed XPS measurements were carried out before and after Ge deposition and annealing on Pt(111). Figure 3 shows the spectra of Pt 4f and Ge 3d. It can be seen from figure 3a that

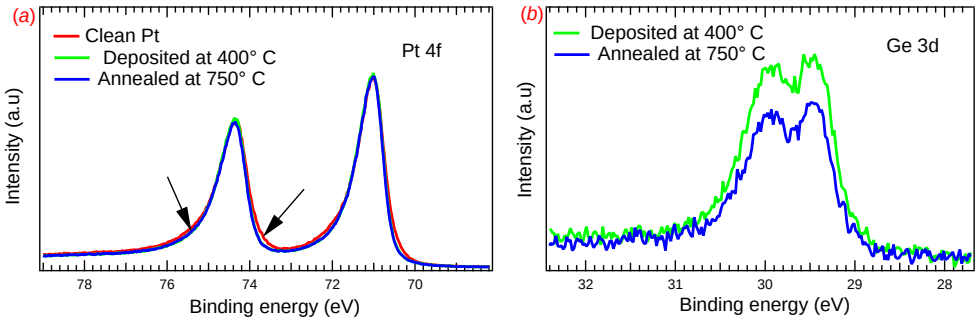

Figure 3. (*a*) Pt 4f XPS spectra for the clean Pt (red), Ge deposited at 400°C (green) and after annealing at 750°C (blue). The arrows show the reduction in the line-width after annealing. (*b*) Ge 3d spectra after deposition at 400°C (green) and after annealing at 750°C (blue).

the positions of the Pt 4f core level peaks remained constant upon Ge deposition, even after annealing to 750°C. However, the width of the peaks decreased after Ge deposition. Generally a decrease in line-width means either a more ordered surface (less chemical environments for the Pt atoms) or an increase in the lifetime of the core-hole produced during the photoemission process. The Pt(111) surface is already very well ordered and it is unlikely that Ge deposition would somehow increase this order. This suggests an increase of the core-hole lifetime. This would most likely result from a reduction in the metallic behaviour of Pt. The absence of a core level shift means that Ge atoms do not affect the state of Pt atoms at the surface. There are two possible explanations for this. The first is that we were in the presence of a GePt surface alloy where the Ge-Pt interaction strength is the same as that of Pt-Pt. This is possible because of the relatively close electronegativity of Pt and Ge (2.28 for Pt and 2.01 for Ge) [15, 16]. Ge-Pt can therefore form a nonpolar covalent bond with electrons localized between the two atomic nuclei. The second explanation is that we had a 2D layer of Ge atoms (germanene) interacting weakly with the Pt surface. In this case, the structure is probably buckled as reported by Li et al [10].

The intensity from the Pt 4f core levels was used to evaluate the thickness of the deposited Ge using the formula $A = A_0 e^{-t/\lambda}$ where A_0 and A are respectively the areas of the clean Pt 4f curve and after Ge deposition, t the Ge thickness and λ the inelastic mean free path of Pt 4f electrons in Ge. This resulted in 0.42 ML just after the deposition, upon annealing it reduced to 0.30 ML. Ge has therefore diffused into the Pt bulk or desorbed into the vacuum of the preparation chamber. Over several experiments we noticed that annealing Pt that has been cleaned by sputtering would result in the appearance of Ge on the surface. Hence Ge atoms diffused into the Pt bulk during the original annealing after Ge deposition. In addition, 750°C is well below the sublimation temperature of Ge in a vacuum. The conversion of the $\sqrt{7}$ structure into the $\sqrt{19}$ structure is therefore driven by a diffusion process.

To gain more insight the Ge 3d core level spectra have been fitted. For both structures, the Ge 3d spectra could be fitted with the same two components (figure 4). This indicated that Ge

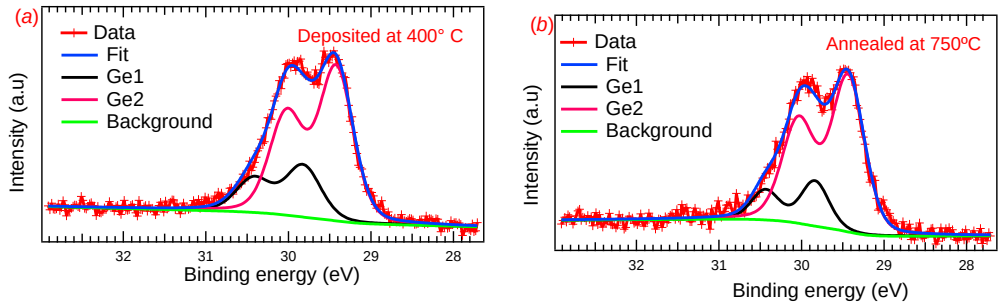

Figure 4. Fits of Ge 3d spectra (a) deposited at 400°C and (b) after annealing at 750°C. The background shown in both panel is a Shirley-type background.

was in the same two different chemical environments. The two components appeared at 29.8 eV (Ge1) and 29.4 eV (Ge2). Their widths were 0.5 eV (Ge1) and 0.48 eV (Ge2). Upon annealing to 750°C, these components did not shift in energy. In contrast their widths decreased upon annealing to 0.47 eV (Ge1) and 0.40 eV (Ge2).

The ratio of the areas of the two components in the Ge 3d spectra was 1:3 for the $\sqrt{7}$ and 1:4 for the $\sqrt{19}$ structure. This rules out unbuckled germanene as in it all the Ge atoms occupy identical sites. Buckled germanene has been reported to either have a 1:1 ratio between the two sites [5], or a 1:5 ratio [10]. In order to better understand the origin of the two sites we looked at the Ge $2p_{3/2}$ core level for the Ge deposited at 400°C, shown in figure 5. The Ge 2p core levels are at a much higher binding energy than the Ge 3d, which means that the 2p photoelectron emitted from the Ge has a much lower kinetic energy. This in turn means that it is substantially more surface sensitive than the 3d levels. Figure 5 clearly shows that the component at higher binding energy was significantly smaller in the surface sensitive regime. In other words, it originated from the bulk, and the component at lower binding energy originated from the surface. The existence of a bulk component is not surprising, given our experience of the diffusion of Ge in Pt. All our evidence pointed towards a Ge-Pt surface alloy. If we look more carefully at the model proposed by Švec et al., we see that the $\sqrt{7}$ structure has more Ge atoms per unit surface area than the $\sqrt{19}$. This agrees with the decrease in surface coverage that we saw with annealing. It suggests that diffusion into the bulk and the resultant lower surface coverage have favoured the formation of the $\sqrt{19}$ structure. The bulk component indicates the existence of a subsurface Ge atom underneath the first layer, possibly below each tetramer. We note that Švec et al. did not see a bulk component in their XPS measurements. This could well be explained by the photon energy that they used, 150 eV, which resulted in an exceptionally

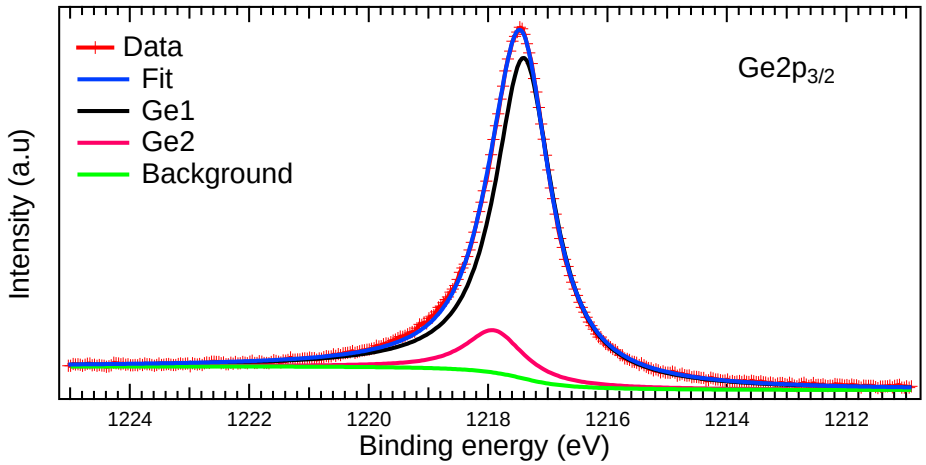

Figure 5. Ge $2p_{3/2}$ spectrum for Ge deposited at 400°C.

surface sensitive measurement.

4. Conclusion

We report that Ge can form a $\sqrt{7}$ or $\sqrt{19}$ structure on Pt(111) depending on the substrate- and annealing-temperatures. This is the first time that Ge with a $\sqrt{7}$ structure has been found experimentally on Pt(111). In both structures the Ge atoms are found to interact weakly with the Pt atoms. From our LEED and XPS analysis, these structures match the Ge_3Pt tetramer model put forth by Švec et al. In addition we found evidence for a subsurface Ge atom. Both the $\sqrt{19}$ structure and the subsurface Ge resulted from the diffusion of Ge into the Pt crystal.

References

[1] Cahangirov S, Topsakal M, Aktürk E, Sahin H and Ciraci S 2009 *Phys. Rev. Lett.* **102** 236804
[2] Dávila M, Xian L, Cahangirov S, Rubio A and LeLay G 2014 *New J. Phys.* **16** 095002
[3] Ye X S, Shao Z G, Zhao H, Yang L and Wang C L 2014 *R.S.C. Adv.* **4** 21216
[4] Liu C, Feng W and Yao Y 2011 *Phys. Rev. Lett.* **107** 76802
[5] Acun A et al. 2015 *J. Phys. Condens Matt.* **27** 443002
[6] Derivaz M, Dentel D, Stephan R, Hanf M C, Mehdaoui A, Sonnet P and Pirri C 2015 *Nano. Lett.* **15** 2510
[7] Golias E, Xenogiannopoulou E, Tsoutsou D, Tsipas P, Giamini S and Dimoulas A 2013 *Phys. Rev.* B **88** 075403
[8] Bampoulis P, Zhang L, Safaei A, Van Gastel R, Poelsema B and Zandvliet H 2014 *J. Phys. Condens Matt.* **26** 442001
[9] Qin Z, Pan J, Lu S, Shao Y, Wang Y, Du S, Gao H and Cao G 2017 *Adv. Mat.* **29** 1606064
[10] Li L, Lu S, Pan J, Qin Z, Wang Y, Cao G, Du S and Gao H 2014 *Adv. Mat.* **26** 4820
[11] Zhang L, Bampoulis P, Van Houselt A and Zandvliet H 2015 *Appl. Phys. Lett.* **107** 111605
[12] Wang Y, Li J, Xiong J, Pan Y, Ye M, Guo Y, Zhang H, Quhe R and Lu J 2016 *Phys. Chem. Chem. Phys.* **18** 19451
[13] Švec M et al. 2014 *Phys. Rev.* B **89** 201412
[14] Meng L, Wang Y -L, Zhang L -Z, Du S -X and Gao H -J 2015 *Chin. Phys.* B **24** 086803
[15] Allen L C 1989 *J. Am. Chem. Soc.* **111** 9003
[16] Mann J B, Meek T L, Knight E T, Capitani J F and Allen L C 2000 *J. Am. Chem. Soc.* **122** 5132